JOURNAL OF MATERIALS SCIENCE 20 (1985) 1455–1465

Toughened polybutyleneterephthalate compounds

Part 1 *Dynamic strains in notched impact test*

F. POLATO
G. Natta Research Centre, Montepolimeri, P. le G. Donegani, 44100 Ferrara, Italy*

The notch sensitivity of polybutyleneterephthalate (PBT) had been improved in a synergistic way, by 30–40 times, by addition of special toughening agents in limited amounts (20–30%). This large toughening effect was studied by high speed photography. Ultimate elongation strain and strain rate at the notch root were measured directly. It was found that the high impact behaviour of toughened PBT is provided by the large amount of plastic strain around the fracture surface. The plastic strain was not observed in the PBT homopolymer during impact fracture, due to its brittle behaviour; on the contrary, it was observed in low speed bending of notched bars. It was concluded that the toughening mechanism of mixed additives is to allow the plastic strain of a PBT matrix at very high strain rates.

1. Introduction

High-impact polybutyleneterephthalate (PBT) compounds are a new family of thermoplastic polyester resins developed in order to improve substantially the poor impact properties of PBT homopolymer in notched tests [1, 2]. The basic requirement was to attain this aim by retaining solvent resistance, mechanical properties and mouldability of PBT as much as possible in order to extend its applicability to objects having sharp corners or other stress-concentration points.

The account of the attained impact strength properties in the technical bullettins and patents were given by reporting the amount of work required to fracture the notched specimen in the Izod or Charpy standard test [3].

The main aim of this study is to provide the experimental evidence of dynamic strains and fracture mode in toughened PBT specimens through the notched impact test by high speed photography [4]. Some hypotheses about the toughening mechanism for this family of thermoplastic compounds will be outlined following from the direct observation of the fracture mode.

2. Experimental procedure

Comparative considerations about equivalence among the various impact tests, useful in order to select the most suitable experimental conditions, are certainly not new. Nevertheless, some basic features of the pure bending impact test are reviewed here for the sake of clarity in approaching the problem.

2.1. Izod–Charpy test comparison

Figs. 1a and b schematically show the well known feature of pure bending in notched Izod and Charpy standard tests [3]. Because of the very high concentration effect caused by the notch, the preliminary assumption is that material strain is constrained entirely in the middle of the specimen bar, around the fracture surface. This assumption will be later confirmed by the photographic evidence. Following the previous statement, the deflection angle Θ of the bar might be calculated in both the Izod and Charpy tests as a function of the striker displacement:

$$\text{Izod } \Theta = \tan^{-1}(s/h) \quad (1)$$

$$\text{Charpy } \Theta = 2\tan^{-1}[s/(2h)] \quad (2)$$

*Now Himont Italia.

0022–2461/85 $03.00 + .12

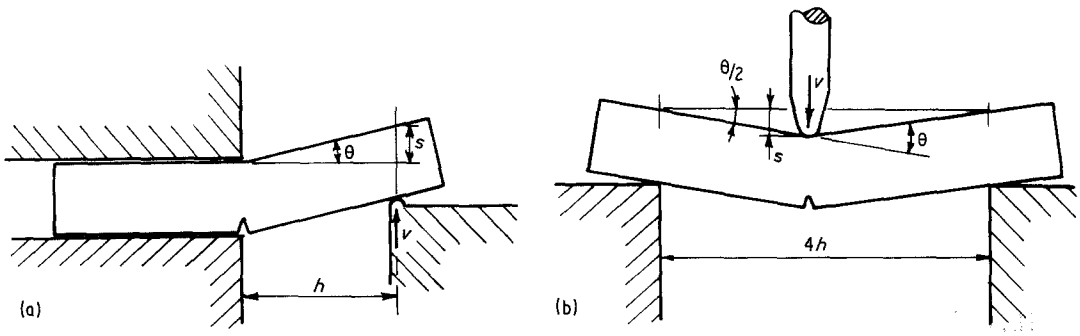

Figure 1 Schematic diagram of (a) bending in the notched Izod impact test; (b) three-point bending in the notched Charpy test.

where s is the striker displacement in the time and h is as defined in Figs. 1a and b. For small angles, usually taken as less than 10°, the approximation $\tan^{-1}\alpha = \alpha$ might be used. Moreover, until the falling weight impact energy is much higher than the mechanical work absorbed by the specimen, the striker displacement in the time might be approximated by the equation:

$$s \cong vt \tag{3}$$

where v is the initial striker impact velocity and t is the time. In this range, Equations 1 and 2 might be rewritten in the following, approximated form:

$$\text{Izod } \Theta \cong vt/h \tag{4}$$

$$\text{Charpy } \Theta \cong vt/h \tag{5}$$

It follows from Equations 4 and 5 that the same bar deflection rate $\dot{\Theta} \cong v/h$ is obtained in both the Izod and Charpy test arrangements when the same v/h ratio is performed. Obviously, this conclusive correlation is allowed for small deflection angles of the bar, within the limits of the previous approximations.

The Izod test was preferred to characterize the impact behaviour of toughened PBT compounds. Nevertheless, some experimental facilities and the higher geometrical symmetry, by which quantitative evaluations are easier to perform, suggest that the Charpy impact test is more suitable than the Izod from the experimental point of view. Moreover, Equations 4 and 5 allow a cross-correlation between the two kinds of impact test, so fracture analysis results might be exchanged from one to the other. These are the reasons why the Charpy arrangement was selected for the present study although both the Izod and Charpy methods should have been used.

2.2. Experimental apparatus

The experimental apparatus consists of a high-speed photography set up assembled on impact equipment. The impact equipment is a falling weight machine in which the specimen support and striker were redesigned in order to reproduce the geometrical features and impact conditions of the Charpy standard test. In other words, the striker impact line is midway between the specimen supports and directly opposite the notch, as in Fig. 1b. A falling weight machine was used instead of the ASTM standard pendulum [3] because of the very poor accessibility to photographic shots in the latter.

Fig. 2 shows schematically the apparatus when operating in the "reflecting mode". The alternative, "transmitting mode", is very similar and will be seen later. The dynamic force resulting from the impact of the striker on the bended specimen is converted into an electrical voltage by FD and recorded by the transient recorder TR (input C1). The dynamic strain mechanism is directly observed by suitable shots of high-speed photography. Both "single-flash" and "multi-flash" techniques are employed, depending on the strain information required. The single-flash technique has been known for many years [4, 5] and allows us to study high speed phenomena by taking a series of single photographs of the observed structure at different successive instants through the phenomenon. In order to do this, a series of identical experiments must be repeated and each experiment is photographed after a particular delay-time. The single photograph is shot by previously opening the photographic carmera PC and illuminating the structure by a strong and very short flash light pulse. In the present apparatus the switch S1 is started by the magnetic rod MR and opens the objective throughout the specimen fracture by the one-shot

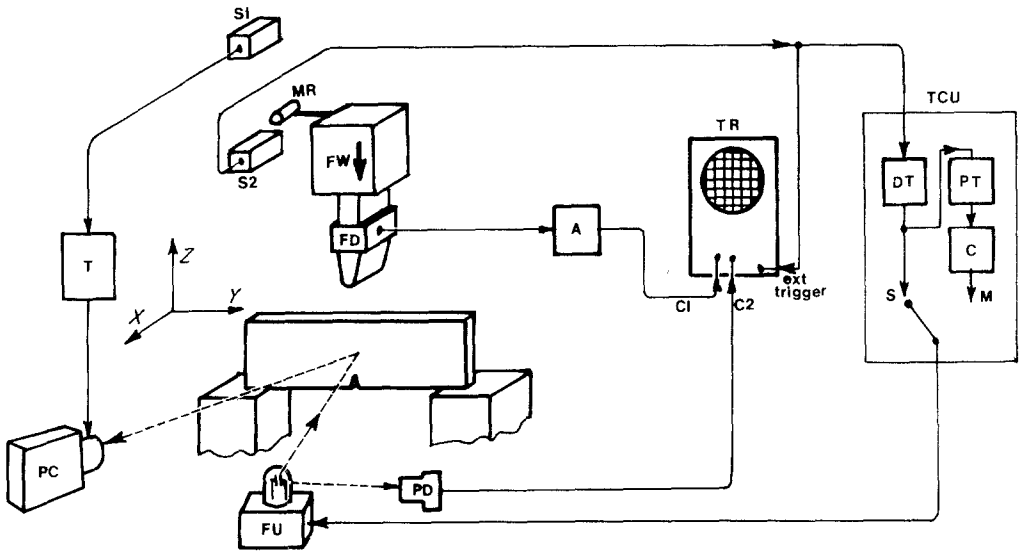

Figure 2 Schematic set-up for high speed photography and stress recording in the Charpy impact test. Reflecting mode and single-flash technique.

timer T; the delay-time for the flash pulse is started in the switch S2, again by MR. The delay-time is tuned by the DT modulus in the time-control unit. With reference to the cartesian axis system *xyz* shown in Fig. 2, the light beam (supplied by the flash unit FU) can lie parallel to the *xz* or to *xy* plane. The narrow spreading of the stress-time diagram in the Charpy test suggests a high order reproducibility of the specimen fracture behaviour through the impact experiment. Moreover, by repeating the photograph over the same impact instant for lots of identical samples, the same deformation field was observed in the bar. Although the specimen must be changed for every photograph because it is a destructive test, the above mentioned experimental evidence allows us to consider a series of single-flash photographs as the replay of a single impact experiment.

The flash pulse is detected by the photomultiplier PD and recorded by TR (input C2). In this way the specimen strain observed by the flash pulse can be unambiguously correlated to the applied stress.

The multi-flash technique is similar to the above described single-flash and is performed by shooting the observed structure more than once during the phenomenon without any change in the photographic apparatus. For this purpose the flash unit is activated by the output M of the time control unit TCU. The train pulse starts after a delay-time (tuned by the DT modulus in TCU) and is interrupted by the fixed count digital counter C when the required number of flashes has been shot. The delay time between two successive flash pulses is tuned by the PT modulus in TCU.

The "transmitting mode" differs from the above described "reflecting mode" only in geometrical features. The flash unit is placed in front of the photographic objective; the specimen is in the middle, all the three lying on the same *x*-axis. The transmitting mode is very suitable when observing the profile deformation of the sample. Some additional data concerning the experiments are the following: the flash light pulses were supplied by a GR 1538A stroboscopic unit. The flash duration at 1/3 peak intensity was 3 μsec in the single-flash technique and 0.8 μsec in the multi-flash. The transient recorder was a Biomation 1015 WR. Photographs were taken by a Linhof objective on Polaroid film (75 ASA). The experimental impact conditions were: specimen support span $4h = 60$ mm; impact mass $m = 2.60$ kg; fall height $l = 0.46$ m; striker edge radius $r = 3$ mm and notch apex radius $R = 0.17$ mm. The striker impact energy (11.7 J) was much larger than specimen fracture energy (2.63 J). The initial impact velocity was 3.0 m sec^{-1} and was checked with the high speed photography equipment. The experimental value was found to be 2.97 m sec^{-1} ± 0.3%.

2.3. Samples

Initially the GUF product Gaftuf 4062/Z was selected for this study from the commercially available toughened PBT compounds. Subsequent steps could be the quantitative comparison of the

different compounds if, from a coarse analysis, it seemed that the impact behaviour of this family of compounds was qualitatively the same.

After a vacuum drying at 120° C for 2 h the resin was injection-moulded at 240° C. The bar specimens (12.7 mm × 3.15 mm sections) were notched following ASTM D256B, section 6 instructions. For the reflecting-mode photography, light was reflected from the observed side of the notched bars by a gold coating. The metallic coating avoids light diffusion by the polymeric bulk (semicrystalline and etherophasic) and makes it possible to observe specimen strains as variations of light intensity reflected by the surface into the objective angle of view. The gold coating was applied by a Semprep P2 Nanotech sputter coater. The amount of gold thickness was only 0.05 μm in order to avoid mechanical contributions of the metallic coating to the polymer impact behaviour. This goal was considered accomplished to the full as no differences were observed by statistically comparing stress–time diagrams of both coated and uncoated specimens. In order to carry out quantitative measurements of the bar surface strain, a square grid was drawn on the metallic coating of some specimens. The square grid was oriented with the major axis of the bar side and the cartesian origin was placed at the notch apex. The grid step was 0.500 ± 0.005 mm.

3. Results and discussion

Fig. 3a shows the stress–time behaviour of the examined material Gaftuf 4062/Z and the time scale positions of photographic shots taken by the multi-flash technique on the impact test. Striker displacement and bar deflection scales are also drawn by the side of the time scale in order to measure directly the amount of bar bending. Specimen impact energy is measured by integrating the stress–time diagram and is about 80 kg cm cm^{-1}. Fig. 3b shows the subsequent bending steps of the bar, strain at the notch root and fracture advance. In order to check Equation 5, bar deflection was measured as a function of time for a lot of specimens and by shifting the flash pulse train in the time. Experimental results are shown in Fig. 4 where it appears that the start of the bar deflection is delayed from striker-bar contact by a fraction of a millisecond. This delay is explained by assuming that some penetration of the metallic supports and striker in the resin bar takes place at first. After this initial and very limited discrepancy, linearity between bar deflection angle Θ and time t is clearly evident. This experimental result is provided by Equation 3b for small angles usually taken as $\Theta < 20°$. The error in the approximation at $\Theta = 40°$ should be 4.3%; at $\Theta = 60°$ should be 11.3%. The observed linearity of Θ versus t up to 60° might be explained by taking into account some compensative effects such as the velocity loss of the falling weight and the curvature of the bar in the impact area. Apart from this lucky experimental facility, the deflection angle Θ depends only on the striker displacement and was assumed to be the independent variable in studying Charpy fracture.

Quantitative measurement of notch and fracture tip radius, elongation strain at the notch root and

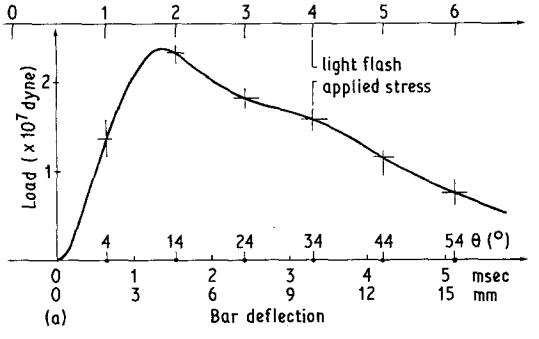

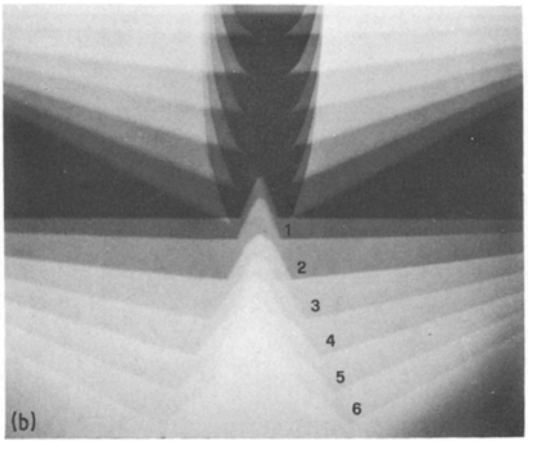

Figure 3 (a) Toughened PBT compound Gaftuf 4062/Z. Impact behaviour in the Charpy notched test and photographic observation instants (with reference to Fig. 3b); (b) Multi-flash shot of the Charpy impact fracture (transmitting mode). Shot number 0–5 correspond to the light flash numbers of Fig. 3a.

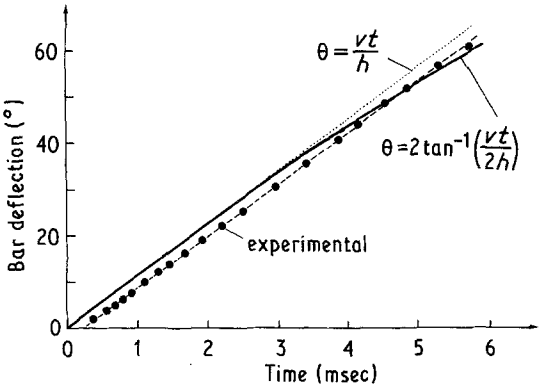

Figure 4 Correlation between time and bar deflection angle (Θ) during the notched Charpy impact test.

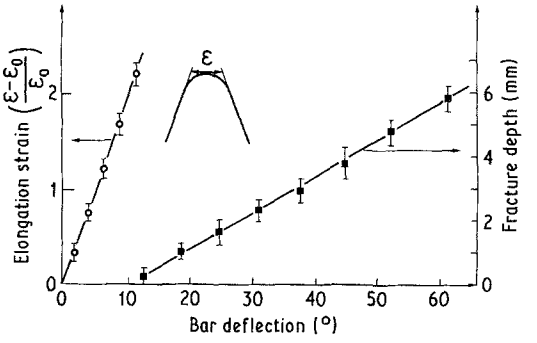

Figure 6 Toughened PBT compound Gaftuf 4062/Z. Elongation strain in the notch root (left side) fracture propagation (right side).

also fracture advance during impact were taken from the above mentioned impact test series and plotted against bar deflection angle Θ. Notch and fracture tip radius were measured by overlapping a series of different radii circles to the enlarged tip picture to find the best agreement. The results are shown in Fig. 5 and allow us to conclude the following: notch radius grows with angular bar deflection up to the maximum load, where it reaches about five times the initial value. It is expected that this large increase in notch radius before the fracture starts is correlated to a large effect in the stress intensity factor. When the ultimate load has been achieved, material fracture starts in the notch root by crack opening. This occurs after a bar deflection of about 12°. The crack radius is very small at the beginning and with the specimen bending growth, at $\Theta \cong 15°$, it quickly reaches about the same value as the man-made notch radius. After that, it increases quite linearly with bar deflection. Elongation strain at the notch before the start of the fracture was measured by

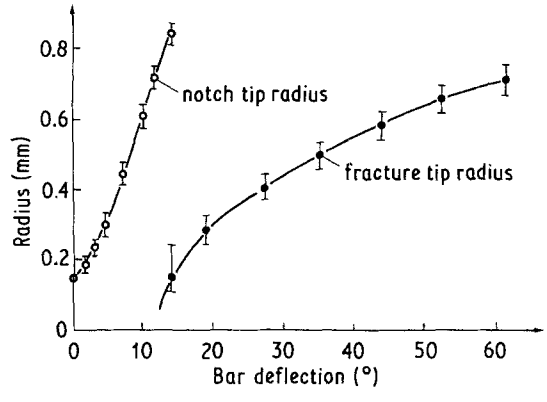

Figure 5 Toughened PBT compound Gaftuf 4062/Z. Notch and fracture tip radius in the Charpy impact test.

the segment drawn from the notch borderline, as outlined on the upper side of Fig. 6, where the obtained results are shown on the left. According to the increasing load, elongation strain increases with sample deflection quite linearly. The observed elongation rate is 2300 sec^{-1}. Ultimate elongation strain $[(\epsilon - \epsilon_0)/\epsilon_0 = 2.3]$ is achieved at the time of the crack opening, when the bar deflection angle is about 12°. Following the previous hypothesis about the strain concentration effect of the notch, it is pointed out that elongation in the notch root is growing more directly with bar deflection than as an effect of material compliance. In other words, the true role of the notch seems to be that of a strain concentrator rather than of a stress concentrator. The strain evidence shown here is very attractive from the experimental point of view as it suggests the use of the notch in flexural impact tests as a suitable tool by which very high strain rates (10^4 sec^{-1}) can be reached using the conventional Charpy impact apparatus in spite of the low impact velocity range (1–10 m sec^{-1}). By considering the measured strain at the notch root, the toughened PBT grows longer for 3.3 times its initial length before the crack opening starts and this growth happens in about 0.001 sec. It is expected that only special grade polymeric structures can support the above mentioned strain rate condition. Moreover, deformation behaviour is not rubber-like because plastic deformation is observed on the fracture surface after impact. It follows that general material yield and plastic flow of the specimen in the notch before the crack opening starts must be considered in order to account for the previous elongation evidence. Direct bulk observations near the fracture, reported later, allow us to exclude that crazing could also act in the

deformation mechanism. Because of the molecular friction during the specimen shear yielding before fracture, it is expected that some amount of impact energy is converted into heat, so increasing the material temperature. Consequently, mechanical properties inside the yielding material might be lowered just before the fracture. This means that behaviour transitions should be considered, in real time, during impact.

Fracture propagation (Fig. 6, right side) was measured on enlarged photographic prints as the complement of the residual bar breadth along the impact line. The crack opening occurs, as stated, at 12° of bar angular deflection. After that, the

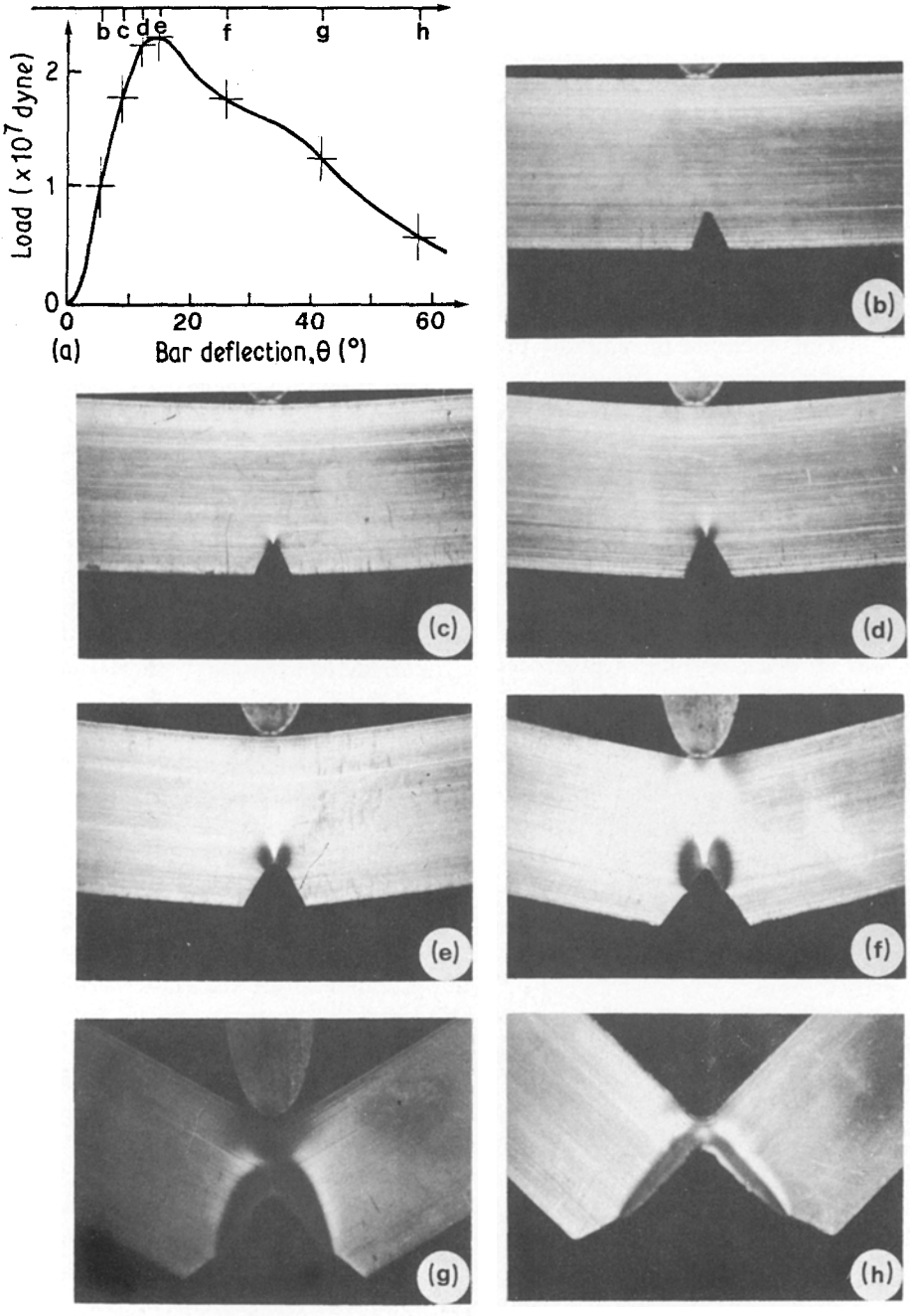

Figure 7 Toughened PBT compound Gaftuf 4062/Z. Single-flash shot of a Charpy impact fracture (reflecting mode). Light beam in *xz* plane (as shown in Fig. 2).

fracture depth increases proportionally with bar deflection and the resulting growth rate is 1.4 m sec^{-1}.

Dynamic strain at the notch root is shown in Fig. 3b. It is emphasized that plastic deformation occurs during impact but no evidence is given of the strained volume amount. In order to produce this further experimental evidence, a series of coated specimen bars were observed during the impact test in the reflecting mode, single-flash technique. Figs. 7b–h show the significant plastic strain steps during the Charpy impact. Corresponding shot times are indicated in Fig. 7a, on the stress–deflection diagram. Picture brightness changes are indicative of surface deflections because of bar

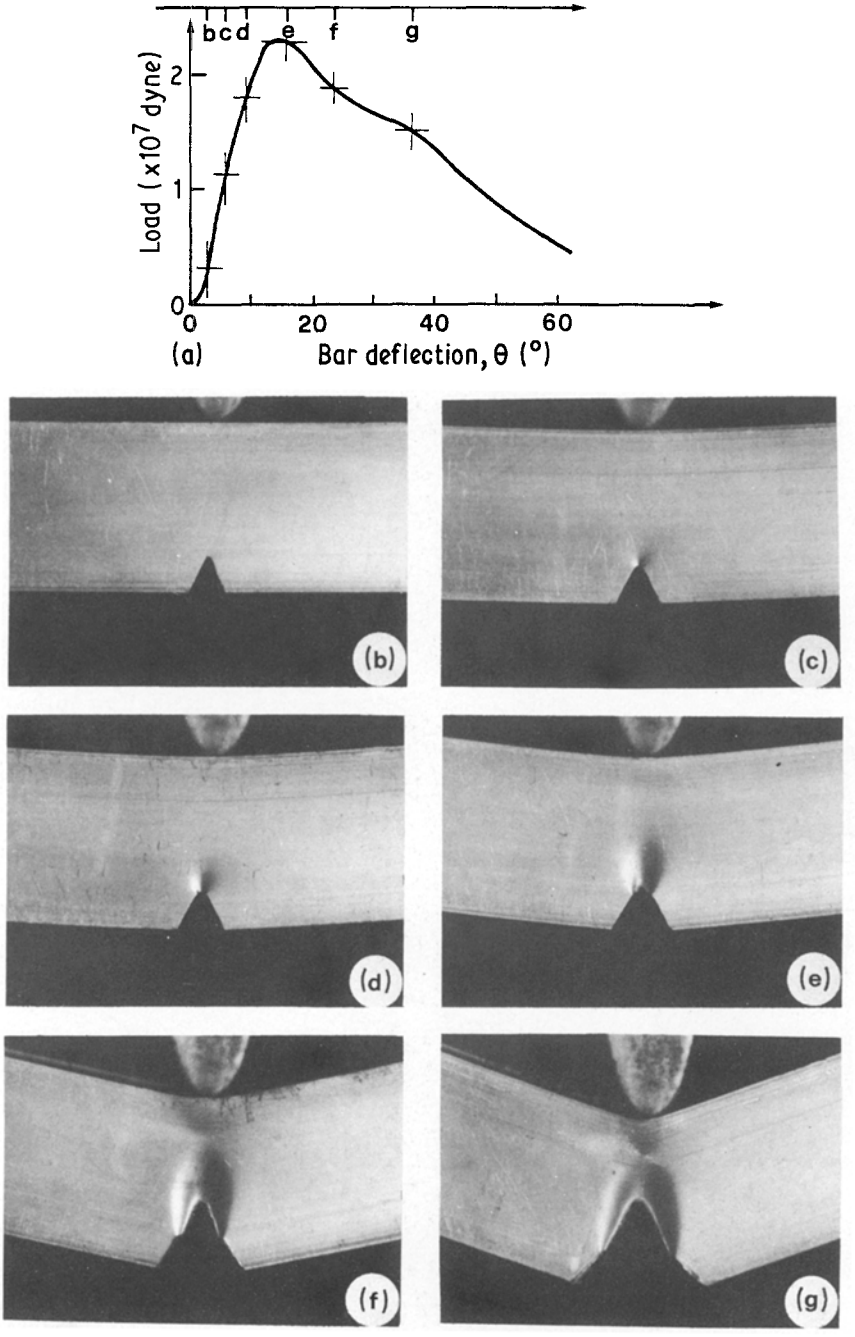

Figure 8 Toughened PBT compound Gaftuf 4062/Z. Single-flash shot of a Charpy impact fracture (reflecting mode). Light beam in *xy* plane (as shown in Fig. 2).

thickness variation. When the thickness change occurs in some amount, it cannot be explained without large deformations. As can be seen in Fig. 7c and d, sample thickness is decreasing at the notch root before of the crack opening starts, according to the previous evidence of large strain (Fig. 6). During fracture propagation, a large amount of deformation is observed in the surroundings of the fracture surface (Fig. 7e–h). Better strain evidence is obtained by enlightening the specimen bar following xy plane, as shown in Fig. 8. It is to be noted that the strained volume boundary line is significantly similar to the slip-line contour of the plastic zone [6, 7] also observed in polycarbonate slow rate fracture. Quantitative measurements of the strained volume width were performed as follows: bar specimens, with a square grid drawn on the coated surface, were photographed at various successive instants in the reflecting mode. Let us consider Fig. 9 as an illustrative example. The strained area was contoured by the grid, which had an initial area (before strain) of A_g and was indirectly measured by counting the number of squares. The strained volume V_s was determined by the equation:

$$V_s = (A_g - A_e)d \tag{6}$$

where A_e is measured directly (Fig. 9) and d is the initial undeformed bar thickness. In this approximation, the external area A_e is assumed undeformed in comparison to the plastically strained area surrounding the fracture, as can be seen from the small amount of planar deformation inside A_e. Moreover, to account for the stretching, the apparent strained volume V_s^0 was determined by the equation:

$$V_s^0 = A_s \times d \tag{7}$$

where A_s is measured directly as shown in Fig. 9. Fig. 10 shows the apparent and effective strained volume V_s^0 and V_s, versus bar deflection during impact. The strained volume growth rate decreases rapidly after the start of the fracture opening, only for the effective strained volume. Unfortunately, plastic-flow field complexity does not enable the direct correlation between the strained volume and the mechanical work carried out by the striker in a simple manner; this is also because the work density per stretched unit volume depends on molecular orientation and so grows with the amount of stretching. Nevertheless, the above mentioned correlation might be attempted in the following, semiqualitative manner:

1. In the first deflection stage of the bar, up to about 4°, mechanical work on the specimen is substantially of elastic nature and shear yielding is not observed. The work of deformation for the bar deflection in this stage is very low: 0.025 J.

2. In the second stage, from $\Theta = 4°$ to 12° of bar deflection, mechanical work is spent to promote general yield and plastic flow at the notch root up to the ultimate stress, where crack fracture starts. The work of the bar deflection in this stage is about 0.5 J.

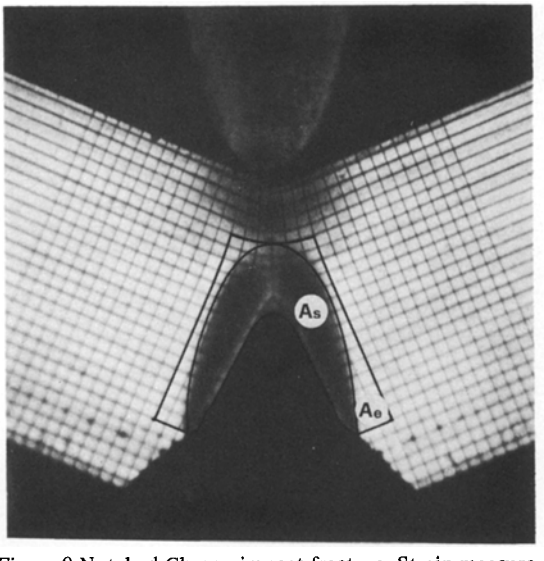

Figure 9 Notched Charpy impact fracture. Strain measurement is by means of the square grid drawn on the coated specimen surface. This high-speed photograph is by the single-flash technique, reflecting mode.

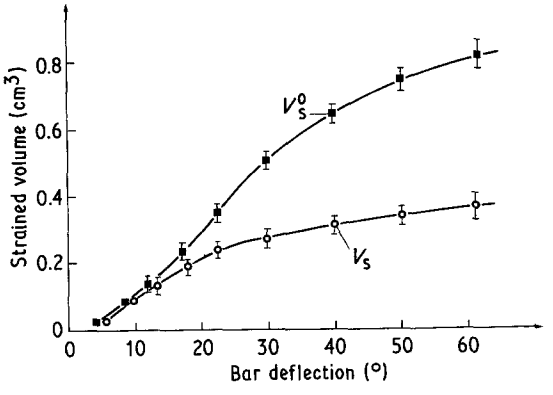

Figure 10 Toughened PBT compound Gaftuf 4062/Z. Strained volume (V_s) and apparent strained volume (V_s^0) during the bar deflection in the notched Charpy impact test.

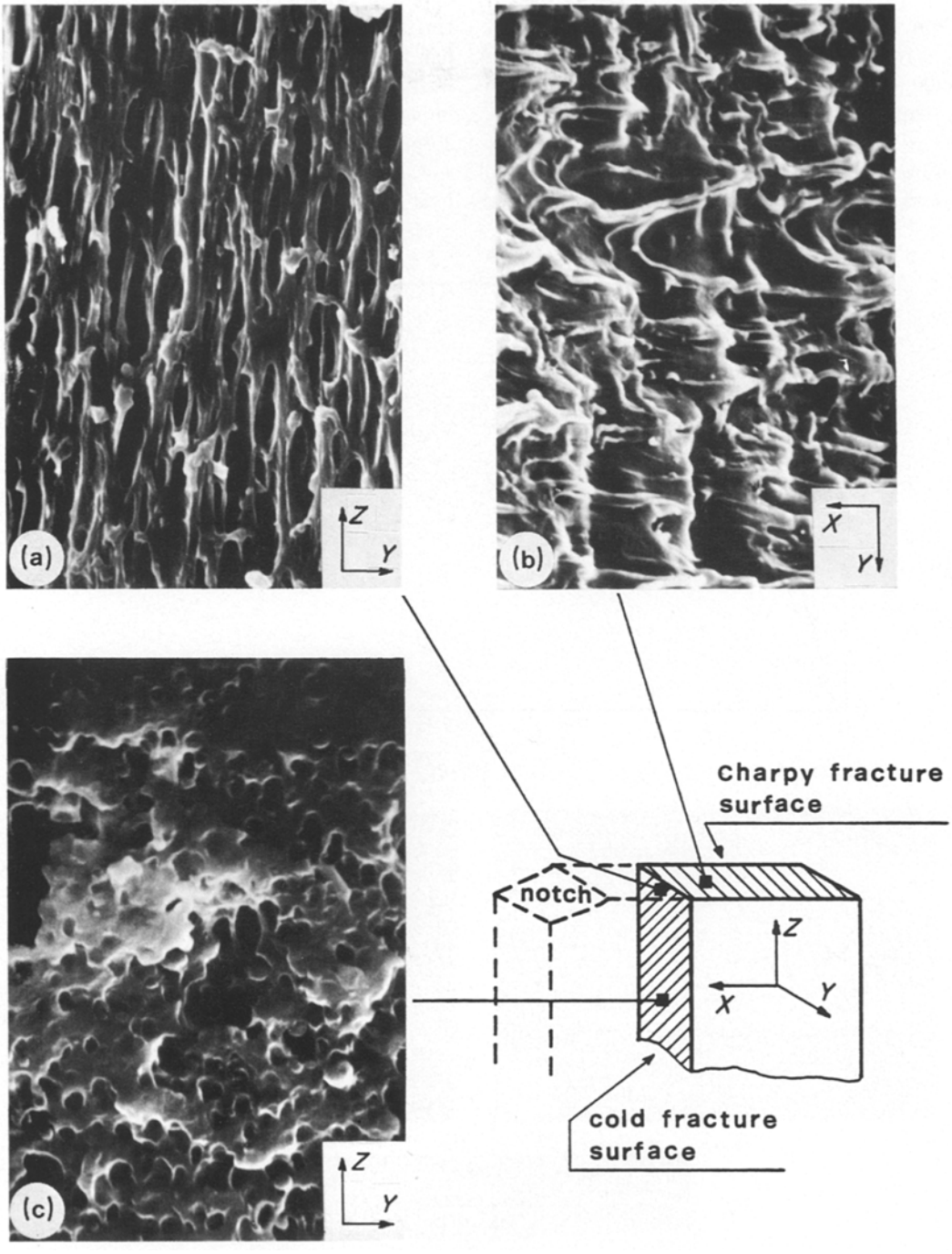

Figure 11 SEM fractography of Gaftuf 4062/Z. (6000 X); (a) stretching under the Charpy fracture surface; (b) fracture surface tearing; (c) bulk morphology.

3. The following stage invloves the effective specimen fracture and requires the largest amount of mechanical work: 2.1 J. It is to be noted (Fig. 10) that the V_s growth rate is substantially lower than in the previous stage while, at the same time, V_s^0 grows at a steady rate. This apparent disagreement is covered by taking into account that the internal shear of the strained volume is of a limited extent during the second, general yield stage, and much more extensive during the tearing for fracture propagation.

Fig. 11 shows some morphological effects related

to the strain behaviour. The bulk morphology (Fig. 11c) is completely stretched in the area surrounding the fracture surface, as can be seen from the ellipsoidal form of cavities near the fracture surface (Fig. 11a). Quantitative aspect ratio measurements of cavities, performed on Fig. 11a, allow us to state that the continuous matrix around fracture is drawn to more than 3.3 times its original length before reaching the fracture. It seems obvious that a large proportion of the overall impact energy required for this plastic work is absorbed into the matrix surrounding the fracture surface and, according to the previous conclusions, heat generation during impact should be evaluated

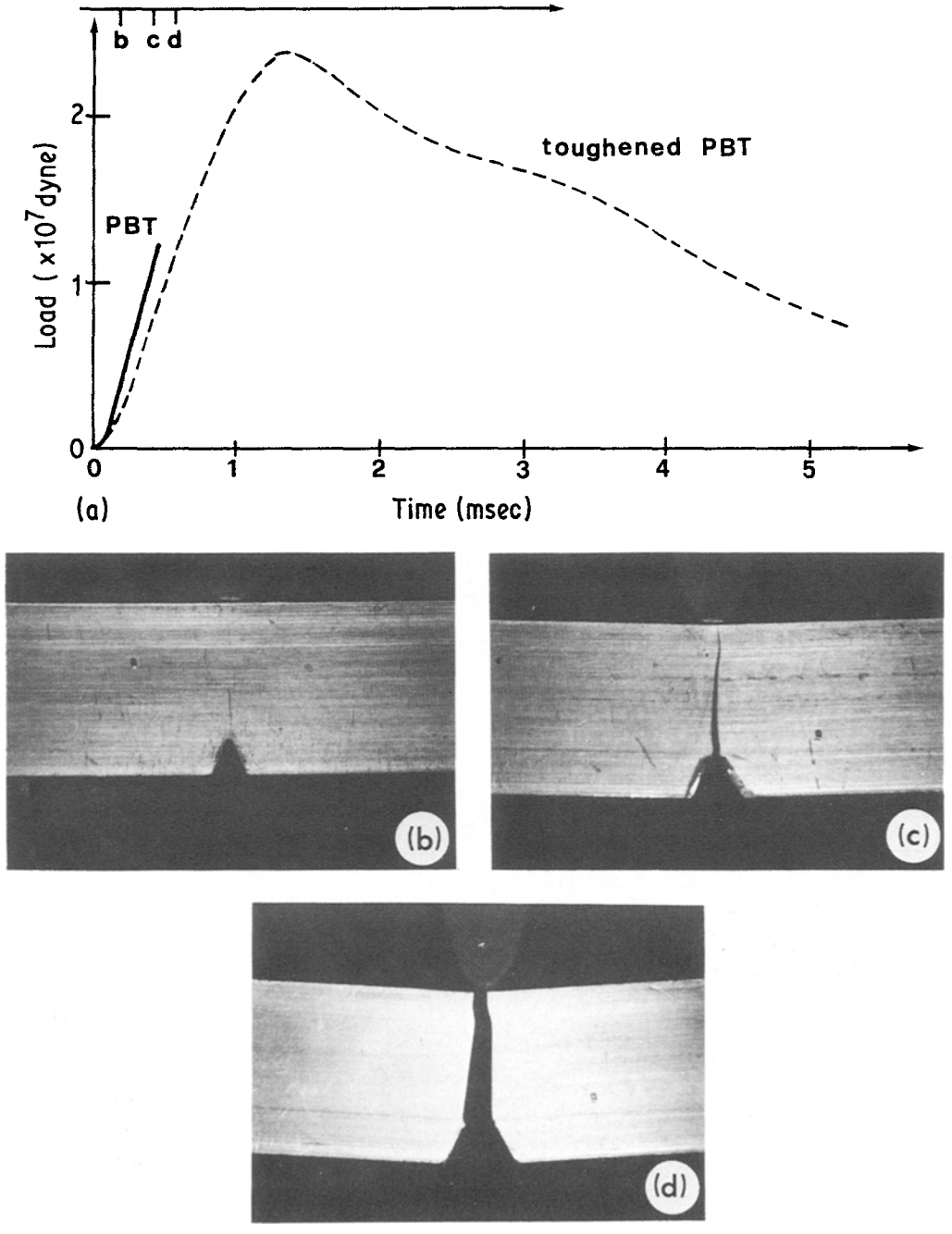

Figure 12 PBT homopolymer. Single-flash shot of the Charpy impact fracture (reflecting mode). Light beam in *xz* plane (as shown in Fig. 2).

for a better material behaviour analysis. As shown by grid distortion (Fig. 9) some amount of elastic strain occurs around the crack fracture opening. Its displacement is clearly driven by the crack advance. It may be expected that elastic energy release, being successive to fracture propagation, does not influence the impact mechanism to a great extent.

Fig. 12 shows the notched impact behaviour of a pure PBT homopolymer, taken as reference. The poor impact energy absorption by the PBT specimen (about 0.15 J) is well explained by the lack of plastic strain, as can be seen in Fig. 12b, where the just-open fracture is shown. From the stress-deflection diagram (Fig. 12a), where Gaftuf 4062/Z behaviour is also shown for comparison, it can be seen that the PBT ultimate load is about one-half that of the toughened compound and PBT brittle fracture occurs at about 2.5° of the specimen bar deflection. At this stage the material general yield at the notch root should begin (Fig. 10) for the ductile fracture. The ultimate elongation strain for the PBT homopolymer, estimated at the notch by Fig. 6 from the maximum bar deflection (2.5°), is no greater than 50%. It appears very low when compared with the Gaftuf 4062/Z value (> 300%). In Fig. 12 the explosive fracture of the specimen can also be seen, with bar pieces being projected away from each another. This explosive effect is explained as following the elastic energy release by the specimen. Experimental measurements could be carried out on this effect for a more accurate fracture energy balance of brittle materials. This is not in the aim of the present work.

The conclusive hypothesis about the toughening mechanism for the examined PBT compounds could be drawn by taking into account that the pure PBT strain behaviour in notched bending at a low deflection rate ($\dot{\Theta} \cong 0.01$ degree sec^{-3}) is identical to that which we observed in Figs. 3, 7, 8 and 9 for the Gaftuf 4062/Z compound in the notched bending at a high deflection rate, during the impact test. When the low deflection rate is applied to the bar specimen, the strain rate at the notch root is about 1.5 sec^{-1}. When the high deflection rate is used, during the impact test, the strain rate at the notch root is raised to the previously noted value of 2300 sec^{-1}. From the previous evidence it follows that toughening additives introduced into the examined compound allow for the plastic strain of a PBT matrix at high strain rates.

4. Conclusions

The strain mechanism during the Charpy notched fracture was observed by high speed photography in toughened PBT compounds and particularly in Gaftuf 4062/Z. The high-impact behaviour exhibited by this new family of compounds originates from the large amount of plastic strain around the fracture surface. General material yield starts at the notch root after about 4° of angular bar deflection, where the elongation strain is a little more than 50%. In this deflection state the pure PBT bar is just broken. The elongation strain rate at the notch root before the fracture starts is directly measured by this photographic technique. The observed value, 2300 sec^{-1}, is surprisingly high when referred to the striker impact velocity, 3.0 m sec^{-1}, but it is well explained by the strain concentration effects performed by the notch. Crack fracture opening is at the notch root when elongation strain is about 330% of the initial length and bar deflection is 12°. Fracture propagation rate is driven by the striker motion and is 1.41 m sec^{-1}. The general yield step required about 20% of the overall impact energy, the remaining 80% being absorbed for plastic strain during fracture propagation. The toughening effect of mixed additives in PBT compounds is to allow the plastic strain of the PBT matrix at high strain rates. It is the authors opinion that high speed photography is a useful tool for quantitative studies of polymer impact behaviour by strain analysis.

References

1. *Plastic. Technol.* **25** (1979) 18.
2. *Plastic World* 70 (1981).
3. Annual Book of ASTM Standard, part 35, p. 95, (1978).
4. C. A. COLE, J. F. QUINLAN and F. ZANDMAN, Proceedings of 5th International Congress on High Speed Photography, Washington, October 17, 1960.
5. L. PIRODDA and A. BERBENNI, Proceedings of the 7th International Congress on High Speed Photography, Zürich, September 12, 1965.
6. R. HILL, "Mathematical Theory of Plasticity", (Clarendon press, Oxford 1950).
7. M. KITIGAWA, *J. Mater. Sci.* 17 (1982) 2514.

Received 29 July 1983
and accepted 12 April 1984